fluids

MDPI

Article

Numerical Investigation of Flow and Heat Transfer from Twin Circular Cylinders Present in Double Forward-Facing Step

Parthasarathy Rajesh Kanna [1,*], Yaswanth Sivakumar [2], G. V. Durga Prasad [3], Dawid Taler [4], Tomasz Sobota [4] and Jan Taler [5,*]

[1] CO_2 Research and Green Technologies Centre, Vellore Institute of Technology, Vellore 632014, India
[2] School of Mechanical Engineering, Vellore Institute of Technology, Vellore 632014, India; yashwanth.s2020@vitstudent.ac.in
[3] Newnestech GmbH, 1220 Vienna, Austria; venkata.durga@newnestech.at
[4] Department of Thermal Processes, Air Protection and Waste Management, Cracow University of Technology, ul. Warszawska 24, 31-155 Cracow, Poland; dawid.taler@pk.edu.pl (D.T.); tomasz.sobota@pk.edu.pl (T.S.)
[5] Department of Energy, Cracow University of Technology, Al. Jana Pawła II 37, 31-864 Cracow, Poland
* Correspondence: rajeshkanna.p@vit.ac.in (P.R.K.); jan.taler@pk.edu.pl (J.T.)

Abstract: A numerical simulation of the circular cylinder as an obstacle in a double forward-facing (DFFS) step was performed. The size and position of the upstream cylinder (c_1) and downstream cylinder (c_2) were varied to explore their role in heat transfer in both laminar and turbulent conditions. Comparative results of the upper and lower half of the downstream cylinder were plotted as results to understand the heat transfer and flow characteristics around the downstream cylinder due to the effect of the upstream cylinder's dimension and position. For Re = 800, when the c_1 is placed near the bottom of the wall, it results in a pair of rear-side symmetrical vortices, and the c_2 cylinder vortices become larger when the c_1 is shifted towards the top wall. Additional flow separation happens adjacent to the steps when c_1 is greater than c_2. These vortices strongly influence the convection heat transfer from the step. However, when Reynolds number (Re) is increased from 800 to 80,000, these vortices' size is decreased. When c_1 moves from 0.375H to 0.75H, the average Nusselt number is increased significantly. Moreover, a hike in Re results in a higher average Nusselt number irrespective of the position of obstacles. The upstream cylinder significantly enhances the Nusselt number when it is placed near the top wall rather than the bottom wall.

Keywords: double forward-facing step; heat transfer; circular cylinder; bluff body; flow analysis

check for updates

Academic Editor: Leonardo Santos de Brito Alves

Received: 2 January 2025
Revised: 5 February 2025
Accepted: 7 February 2025
Published: 12 February 2025

Citation: Kanna, P.R.; Sivakumar, Y.; Prasad, G.V.D.; Taler, D.; Sobota, T.; Taler, J. Numerical Investigation of Flow and Heat Transfer from Twin Circular Cylinders Present in Double Forward-Facing Step. *Fluids* **2025**, *10*, 48. https://doi.org/10.3390/fluids10020048

Copyright: © 2025 by the authors. Licensee MDPI, Basel, Switzerland. This article is an open access article distributed under the terms and conditions of the Creative Commons Attribution (CC BY) license (https://creativecommons.org/licenses/by/4.0/).

1. Introduction

Stepped flow has been an interesting topic over decades due to its complex flow pattern created by the changes in geometry. Numerous simulations and experimental studies were published on double forward-facing step (DFFS) with turbulent flow, nanoparticles, obstacles, etc.; still, it is a trending topic to investigate as it has versatile applications such as electronic cooling, engines, heat exchangers, thermal circuits, etc. The numerical study of H. Togun et al. [1] on double forward-facing step turbulent flow with the nanoparticle of Al_2O_3 concluded that heat transfer of DFFS is directly proportional to the Reynolds number and percentage fraction of the nanoparticle; moreover, the peak value of the local Nusselt number was observed over the second step, which is way larger than the first step. A. Sh. Kherbeet et al. [2] conducted an experimental and numerical study of micro-scale

forward-facing step flow with nanofluid of Al_2O_3 and SiO_2 with distilled water as a base fluid; the numerical and experimental study results had good agreement and conveyed that the 1% volume fraction of SiO_2 had 30% enhancement in the average Nusselt's number compared to that of distilled water and Al_2O_3. Albdoor et al. [3] concluded through a parametric numerical study of DFFS, where distance between steps is the parameter, that for turbulent flow, the maximum Nusselt's number was observed at the maximum distance between the step and the highest Reynolds number. A numerical investigation by Yilmaz and Oztop [4] on DFFS with step height and Reynolds number as the parameter for turbulent flow explained that the second step of DFFS contributes more to heat transfer and fluid flow; thus, by controlling the second step, the heat transfer and flow characteristics of DFFS can be controlled. A numerical study by Oztop et al. [5] found that the aspect ratio of square cylindric obstacles in a DFFS turbulent flow is directly proportional to the pressure drop and heat transfer, whereas heat transfer is inversely proportional to step height.

Similarly, enhancement of the DFFS with a square obstacle with Taguchi's S/N (signal-to-noise) analysis was numerically performed by Janani et al. [6]; dimension of obstacles, position of obstacles, channel height, and Reynolds number were the control parameters to determine the maximum heat transfer through S/N analysis; and the results of this numerical analysis state that the effect of step height on heat transfer is 79%, which is more than the effect of heat transfer by Reynolds number that contributes only 19% of the heat transfer effect. A numerical study on DFFS with a circular cylindrical obstacle by Barman and Dash [7] explained that all position ratios enhanced heat transfer except Pr = 0.2, and the maximum Nusselt's number was observed at 40% of the inlet as the vertical position of the obstacle. A numerical simulation by Togun et al. [8] revealed that in a DFFS with water as the fluid, the trends in Nusselt number were the same for different dimensions unless the Reynolds number changed; maximum heat transfer was identified for the maximum Re, step height, and temperature difference. Stuer et al. [9] experimentally observed flow physics and vortex generation in a forward-facing stepped flow; the results of the experiment were also compared with published papers by Werner and Wengle [10], Freitas and Street [11], and Dimaczek et al. [12]. A review of convection over step flow was performed by H. A. Mohammed et al. [13], which includes results of incline stepped flow, nanofluids over steps, and numerical and experimental investigation of backward-facing stepped flow; this comparative study concluded that the Nusselt number is directly proportional to step height, velocity, Prandtl number, and aspect ratio, whereas on the other hand, it is inversely proportional to the expansion ratio, reattachment length increases until expansion ration is less than 2.25, and it decreases when the expansion ratio increases to more than 2.25. Similarly, Abu-Mulawesh [14] carried a review on both forward- and backward-facing stepped flow with laminar mixed convection that explains the effect of step height, Reynolds number, temperature difference, aspect ratio, and buoyancy force; it concludes by stating the demands of the forward-facing stepped flow study and 3D laminar mixed convection study which have numerous applications, whereas the studies over them were very minimal. The results of a large eddy simulation of the frigate shape model in a backward-facing step flow published by Rao et al. [15] explain asymmetric flow behavior and bistable flow state with the effect of the cavity on the recirculation length. McQeen et al. [16] performed an experimental analysis of forced convection on a double backward-facing step with a jet over the first step. The effect of periodic forcing on the overall flow characteristics of DBFS was analyzed, which describes that in low-frequency forcing, the pressure above the first step decreases, and the pressure above the second step also increases; when the distance between steps is more than 2.5 times the inlet, the DBFS behaves like BFS. The effect of control rods on the wake of a square cylinder was experimentally studied by Chauhan et al. [17] for different positions of control rod

parameters such as recirculation length, time average drag-coefficient, Strouhal number, Reynolds stress, etc., and they were able to reduce 22% of the square cylinder drag by positioning the control rods. Abbasi et al. [18] carried out a numerical simulation to understand the behavior of the passive wake control of a square cylinder by a flat plate, and the study reveals that only if the control plate length is more than 7.5 times that of the square side can the wake be completely controlled, and the percentage reductions of the drag coefficient, Strouhal number, RMS value of drag, and lift coefficient were 23.5%, 100%, 84.6%, and 99.5%. Moreover, initially, for smaller values of plate lengths, an unsteady flow can be seen; as the length increases slowly, unsteadiness degrades and attains a steady state. Wang et al. [19] conducted a numerical simulation of crossed Poiseuille low-Reynolds-number flow over a circular cylinder to explain the heat transfer for the following parameters: Reynolds number, aspect ratio, and position of the circular cylinder. The study reveals that at a particular Reynolds number, the flow pattern created by the combination of the expansion ratio and position is responsible for the heat transfer characteristics; and for a particular expansion ratio and position combination, the time average Nusselt's number is directly proportional to the Reynolds number. The effect of geometry in unsteady forced convection over backward- and forward-facing steps was numerically studied by Xie and Xi [20], through which it was identified that flow fluctuation can be seen for lower wall lengths to be 10 to 14 times that of the inlet height, the fluctuating frequency is inversely proportional to the step height, and it was also observed that this fluctuation has a positive effect on heat transfer. A review on flow over a bluff body at a moderate Reynolds number carried out by Lekkala et al. [21] gives a clear understanding of the behavior of wake behind the bluff body and how it is affected by different shapes. The study mainly focused on elliptical and circular bluff bodies and compared their position, location, and shape as parameters, concluding that a lot of studies are still required for analyzing flow over circular cylinders at a high Reynolds number. Narayanan et al. [22] observed the effect of an oscillating square cylinder on a laminar flow by numerical simulation, in which the Reynolds number, frequency ratio, phase difference, and rotational amplitude were the parameters for the comparison of results; as a conclusion, it documented that at a low Reynolds number, the drag coefficient becomes less sensitive to the parameters, and a direct proportionality was observed between the frontal area, vortex pattern, and drag coefficient. In Zhang's [23] thesis of high-Reynolds-number flow around the different cylinders and comparison of the results of the different turbulent models, they concluded that the k-k_1-ω model's results were in good agreement with the experimental results; particularly, lift crises of the arc cylinder were accurate with experimental paper of Bot et al. [24]. Xu et al. [25] have documented results of the effect of channel dimensions on the flow around a square cylinder, which explains why the increase in vortex shedding can be seen when the gap is less than 3.5 time that of the inlet; it also states that there is no correlation between boundary condition, Reynolds number, and vortex shedding frequency. A 3D unsteady numerical simulation of flow around a square cylinder subjected to suction and blowing concluded that suction affects the flow more, and shedding changes from symmetric to asymmetric. In contrast, the aspect ratio changes wake structure from steady to unsteady; moreover, aspect ratio 4 changes from dipole to quadrupole; these conclusions were drawn by Rastan et al. [26] with aspect ratio and secondary flow ratio as parameters. The DFFS is very common in electronics cooling, turbine blade cooling, heat exchangers, etc.

To enhance the heat transfer, passive methods should be attempted to save on the cost of cooling. When obstacles are placed in the mainstream flow, it will affect the forced convection heat transfer. Moreover, the downstream vortices of obstacles play a vital role in enhancing heat transfer. A pair of cylinders is introduced upstream of the DFFS. Furthermore, if steps exist then, a complex flow physics is expected. Thus, the DFFS's

interaction with circular obstacles has been gaining interest for the present investigation. The size of the obstacle will have influence, and the flow's Reynolds number should be varied to explore the heat transfer behavior. The present investigation aims to find the role of symmetrical and asymmetrical blocks in the mainstream flow.

Past studies on the DFFS cover a lot, but many different cases still have yet to be studied; in comparison to practical applications of the DFFS, very few studies have been carried out. Only laminated data about simulation are available. Most simulations have lower-order accuracy because of low computation power. Almost all the DFFS numerical studies with obstacles are analyzed by focusing on enhancing the stepped wall's heat transfer characteristics. In contrast, in a DFFS flow, the heat transfer of obstacles will behave differently from the normal duct; moreover, if there are two obstacles in a DFFS flow, then their heat transfer will get affected by each other as well as by the DFFS. This type of study opens new flow and heat transfer problems in the famous DFFS flow, which helps develop new DFFS applications.

2. Methods

2.1. Geometry of the Problem

The dimensions of DFFS are fixed where H is inlet height 0.02 m, total length of DFFS L is $40H$. Step heights h_1 and h_2 are equal at $0.25H$, and step lengths a and b are $5H$ and $10H$, respectively. The diameter of cylinders are d_1 and d_2, respectively, which are chosen as different combinations of $0.2H$ and $0.4H$ for d_1 and d_2, which results in 4 different combinations of c_1 and c_2. Position of c_2 is x_2 and y_2 which is fixed, $y_2 = (H - h_1)/2$ and x_2 is H; it is chosen that the velocity profile of c_1 interferes with c_2 in all cases. The position of c_1 is x_1 and y_1 where x_1 is equal to x_2, and y_1 position has 2 cases which are $y_1 = y_2$ and $y_1 = 2$ times of y_2. The various symbols used in the manuscript are listed in Table 1. The schematic of the problem is shown in Figure 1.

Table 1. Symbols used and their abbreviations.

Nomenclature	
a	length of fin, m
b	position of fin, m
c	height of 1st step, m
C	constants
C_p	specific heat $\frac{\mathrm{J}}{\mathrm{kg \cdot K}}$
d	height of 2nd step, m
d_1, d_2	obstacle diameter, m
D_h	hydraulic diameter, m
F_h	height of the fin, m
F_p	position of fin, m
G_k	kinetic energy generated, J
H	duct inlet height, m
h	convective heat transfer coefficient, $\frac{\mathrm{W}}{\mathrm{m^2 \cdot K}}$
h_1, h_2	step height, m
k	thermal conductivity, W/m K
K	turbulent kinetic energy, $\mathrm{m^2 s^{-2}}$
L	total length of duct, m
Nu	Nusselt number
p	pressure, Pa
Pr	Prandtl number

Table 1. *Cont.*

Nomenclature	
q	heat flux, $\frac{W}{m^2}$
Re	Reynolds number
T	temperature, K
u	x direction velocity vector, $\frac{m}{s}$
v	y direction velocity vector, $\frac{m}{s}$
x	x coordinate
y	y coordinate
λ	coefficient, Wm^2/kgK
ρ	density, $\frac{kg}{m^3}$
μ	dynamic viscosity, Pa·s
μ_k	kinematic viscosity $\frac{m^2}{s}$
μ_t	turbulent dynamic viscosity, ($kgm^{-1}s^{-1}$)
ε	dissipation rate, $\frac{m^2}{s^3}$

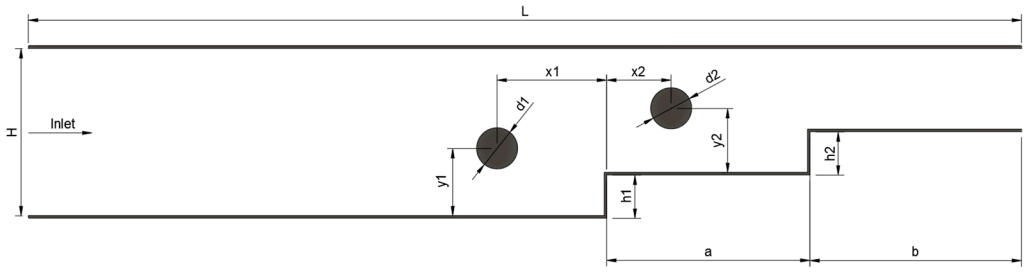


Figure 1. Schematic of the problem.

Different cases will be created by different combinations of y_1, c_1, and c_2. There are two cases of y_1 along with 4 cases of c_1 and c_2; in total, there are 8 cases for the geometry of the problem. In addition, the study is also for comparison of different Reynolds numbers (Re). Reynolds numbers which are considered for study are 200, 800, 20,000, and 80,000, so a total of 32 different cases are compared.

The main objective of this investigation is about the effect of cylinder c_1 on cylinder c_2. All the heat transfer results are taken on the surface of cylinder c_2 for different Re, y_1 and d_1.

2.2. Mathmetical Formulation

The finite volume method, which is used in the commercial program ANSYS 2023 R1 is used to solve the governing equations of the two-dimensional incompressible turbulent flow studied in this numerical simulation. The kinetic energy (k) and dissipation (ε) model is used to compute the turbulent viscosity (μ_t). The mass, momentum, and energy conservation are shown in the following equations. SIMPLE solves the mathematical equation for 10^{-6} residual pressure velocity coupling. The governing equations for the problem considered here are as follows [7].

Continuity

$$\frac{\partial \overline{u}_j}{\partial x_j} = 0 \tag{1}$$

Momentum

$$\frac{\partial(\rho \overline{u}_i \overline{u}_j)}{\partial x_j} = -\frac{\partial}{\partial x_i}\left(\overline{p} + \frac{2}{3}\rho k\right) + \frac{\partial}{\partial x_j}\left[(\mu + \mu_t)\frac{\partial \overline{u}_i}{\partial x_j}\right] \tag{2}$$

Energy

$$\frac{\partial(\rho\overline{u}_j\overline{T})}{\partial x_j} = \frac{\partial}{\partial x_j}\left[\left(\frac{\lambda}{C_p} + \frac{\mu_t}{Pr_t}\right)\frac{\partial\overline{T}}{\partial x_j}\right] \tag{3}$$

Since the *k*-ε turbulence model is related to *k* and ε and uses the eddy viscosity, it is the most often used model in computational fluid dynamics to derive mean flow parameters for turbulent flow regimes. Using two transport equations given by Launder et al. [27], it is a two-equation model that provides a general explanation of turbulence.

The equation for turbulent kinetic energy (*k*) is given in Equation (5)

$$\frac{\partial}{\partial x_j}(\rho k\overline{u}_j) = \frac{\partial}{\partial x_j}\left[\left(\mu + \frac{\mu_t}{\sigma_k}\right)\frac{\partial k}{\partial x_j}\right] + G_k - \rho\varepsilon \tag{4}$$

The equation for turbulent kinetic energy (*k*) is given in Equation (5)

$$\frac{\partial}{\partial x_j}(\rho\varepsilon\overline{u}_j) = \frac{\partial}{\partial x_j}\left[\left(\mu + \frac{\mu_t}{\sigma_\varepsilon}\right)\frac{\partial\varepsilon}{\partial x_j}\right] + \frac{\varepsilon}{k}(C_{1\varepsilon}G_k - C_{2\varepsilon}\rho\varepsilon) \tag{5}$$

where

$$\mu_t = \rho C_\mu \frac{k^2}{\varepsilon}, \tag{6}$$

$$G_k = \mu_t\left(\frac{\partial\overline{u}_i}{\partial x_j} + \frac{\partial\overline{u}_j}{\partial x_i}\right)\frac{\partial\overline{u}_i}{\partial x_j} - \frac{2}{3}\rho k\delta_{ij}\frac{\partial\overline{u}_j}{\partial x_i} \tag{7}$$

where μ_t is turbulent viscosity and G_k is kinetic energy generated due to turbulency. The values 1.44, 1.92, 0.09, 1.0, and 1.3 are represented by $C_{1\varepsilon}, C_{2\varepsilon}, C, \sigma_k,$ and σ_ε for the constants and turbulent *Pr* number of *k* and ε.

$$Nu = \frac{hD_h}{k} \tag{8}$$

$$Re = \frac{\rho u D_h}{\mu} \tag{9}$$

Equations (8) and (9) are used to calculate the Nusselt number and Reynolds number, respectively, where *u* is the inlet velocity and D_h is the hydraulic diameter of the channel. For the present numerical 2*D* DFFS problem, the height of the inlet *H* is considered as the hydraulic diameter which is equal to 0.02 m.

2.3. Boundary Condition

The chosen boundary conditions are versatile for different applications as air has been used as the flow fluid. The heat flux on c_1 and c_2 can be heat flux generated by electricity or any other component. The constant temperature of the hot bottom wall involves heat transfer and makes the problem interesting to study, along with that of the top wall. Operation was at atmospheric pressure which was equal to 101,325 Pa. Turbulence applied at the inlet and outlet is 5% turbulent intensity and turbulent viscosity ratio as 10.

Table 2 lists about the boundary conditions followed in this problem.

Table 2. Boundary condition of present problem.

Top Wall	***T* = 300 K, No Slip**
Velocity Inlet	Velocity based on *Re*, *T* = 300 K
Pressure Outlet	0 Pa gauge pressure
Bottom wall including steps	*T* = 350 K, No slip
Obstacle c_1 and c_2	q = 5000 W/m^2

2.4. Numerical Method and Valudation

The present mathematical model and numerical method is validated for 6 different cases in 2 different published papers. Figure 2 illustrates the agreement of the present model results with the results of the numerical simulation of DFFS with circular obstacles by Barman and Dash [7] published in 2018. Figure 3 shows the validation result of case 6 in the 2006 published research paper by Yilmaz and Oztop [4]; the paper is a simple turbulent flow in DFFS where the dimensions are varied as parameters and the local Nusselt number has been plotted. The validation shows that the results of the present model and published results are almost same.

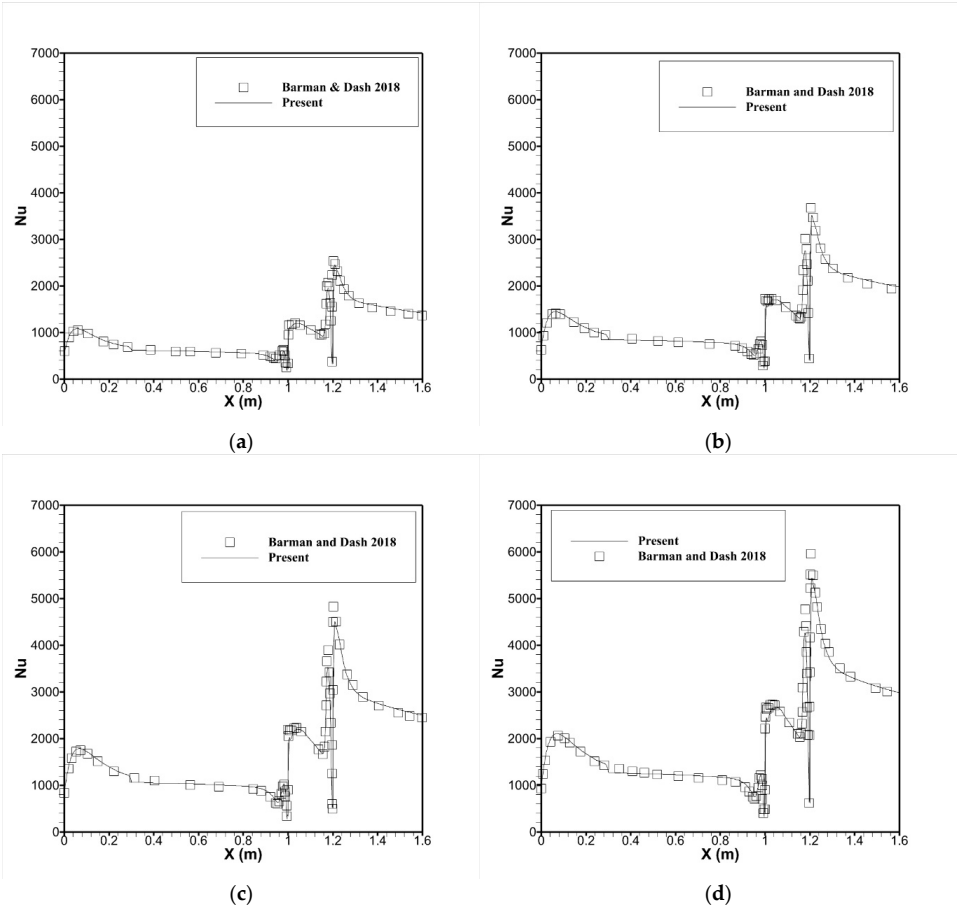


Figure 2. Validation results, case 1 of Barman and Dash's [7] paper; (**a**) *Re* = 40,000, (**b**) *Re* = 60,000, (**c**) *Re* = 80,000, and (**d**) *Re* = 100,000.

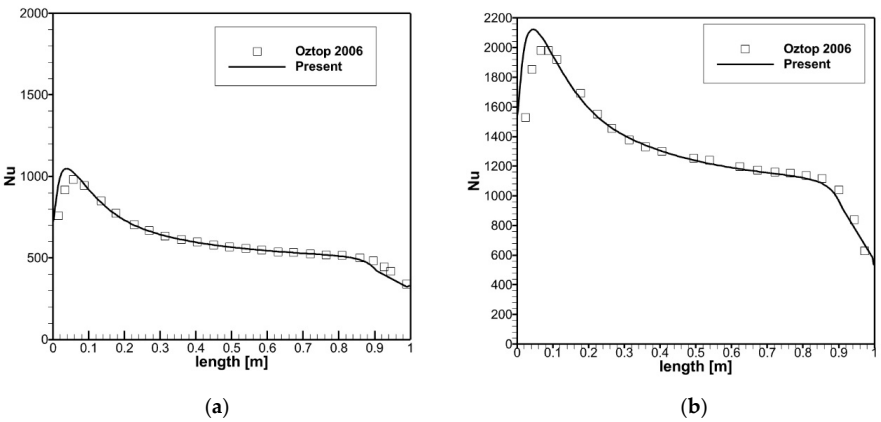


Figure 3. Validation results; case 6 of Yılmaz and Öztop's [4] paper; (**a**) *Re* = 30,000 and (**b**) *Re* = 80,000.

A grid independence study has optimized the simulation setup of the present problem statement to give an accurate solution for optimum computation power.

Based on the grid independence study (Table 3), 74,376 grid count is chosen as it has an error percentage of nearly 0.01%. In Ansys FLUENT meshing, 0.0005 m mesh size with 2 times refinement near bottom wall (including step) and obstacle is used. Figure 4 shows the image of the grid used for the present simulation of 2D DFFS with circular cylindrical obstacles.

Table 3. Grid independence study of present problem statement.

Grid Count	Avg. *Nu*	Δ*Nu*
5984	1610.48	-
13,478	1600.86	0.60388
23,804	1593.56	0.45825
37,771	1587.26	0.39547
74,376	1583.08	0.26239
149,742	1582.91	0.01067

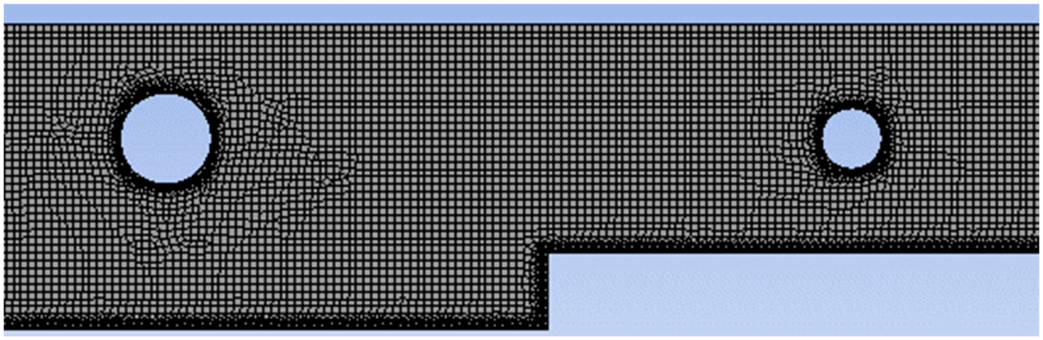


Figure 4. Mesh used for simulation.

3. Results

Double forward-facing step (DFFS) flow with cylindrical obstacles near steps has been investigated numerically for both turbulent and laminar flow. A cylinder (c_1) has been placed in upstream near the first step, whose diameter and vertical position are varied to understand the changes in heat transfer on downstream cylinder (c_2) which is over the first step. Local Nusselt numbers over the upper half and lower half of cylinder c_2 have been compared for different cases. The change in the *Nu* over c_2 is plotted across fraction of diameter, where in all the graphs "(i)" is considered as the upper half, whereas "(ii)" is considered as the lower half of the c_2 cylinder.

The effect of temperature accumulation due to recirculation and its effect on the heat transfer of c_2 can be observed in Figures 5 and 6 for different dimensions and locations of c_2 and c_1. In all the above cases of *Re* and different positions of y_1, it was observed that high Re has more heat transfer compared to low *Re*. This is because a low *Re* creates more recirculation zones apart from the wake behind the cylinders, and even wake behind cylinder is also larger than high *Re*. Recirculation results in an accumulation of heat over that region and as a result, temperature rise can be observed locally over those regions; by the flow of DFFS, this high temperature zone reaches cylinder c_2, which affects the heat transfer. This is one of the main reasons for high *Re* having low heat transfer. At very high *Re*, it is observed there is a sudden reduction in wake after crossing critical *Re*, which greatly helps in the heat transfer of cylinder c_2.

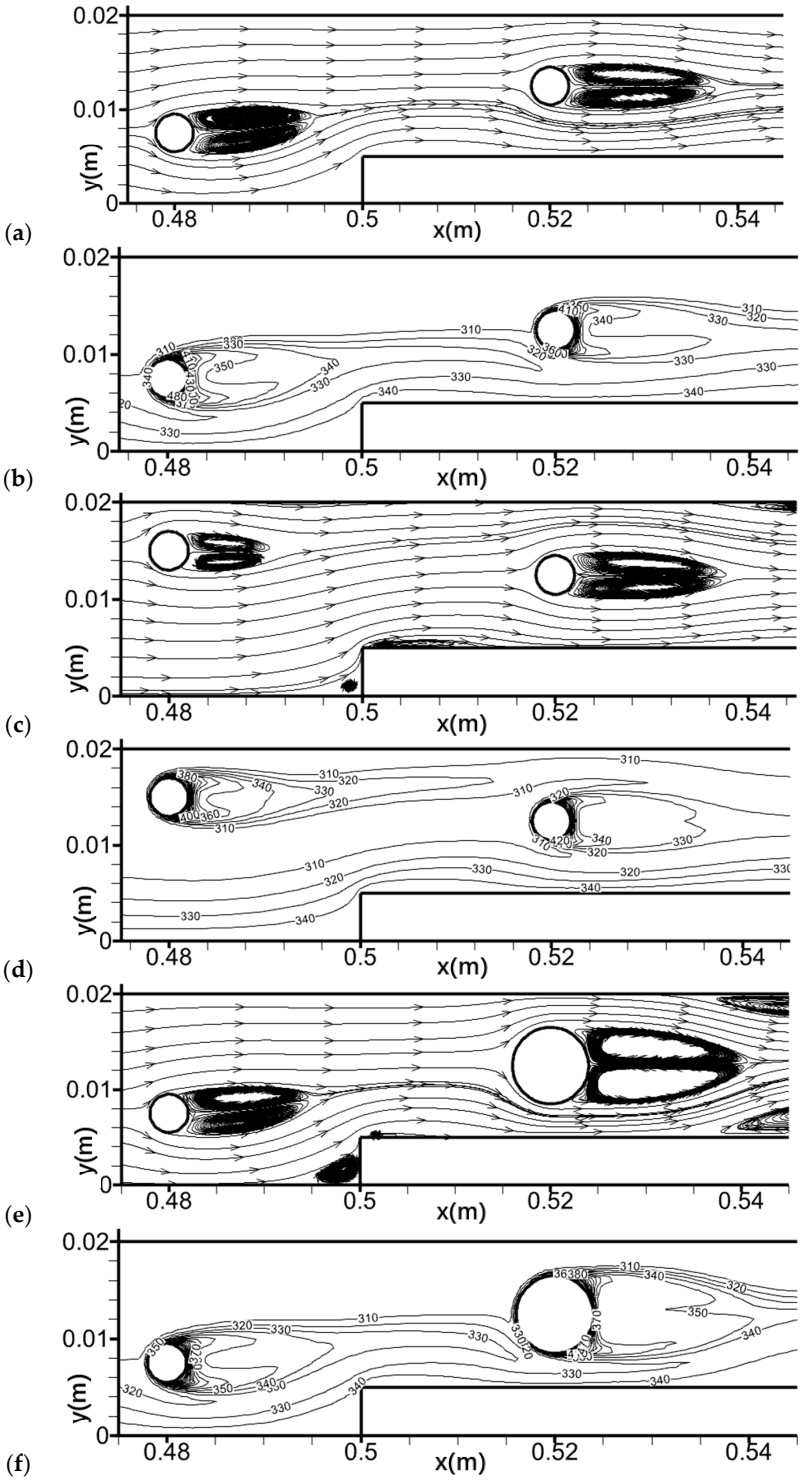


Figure 5. *Cont*.

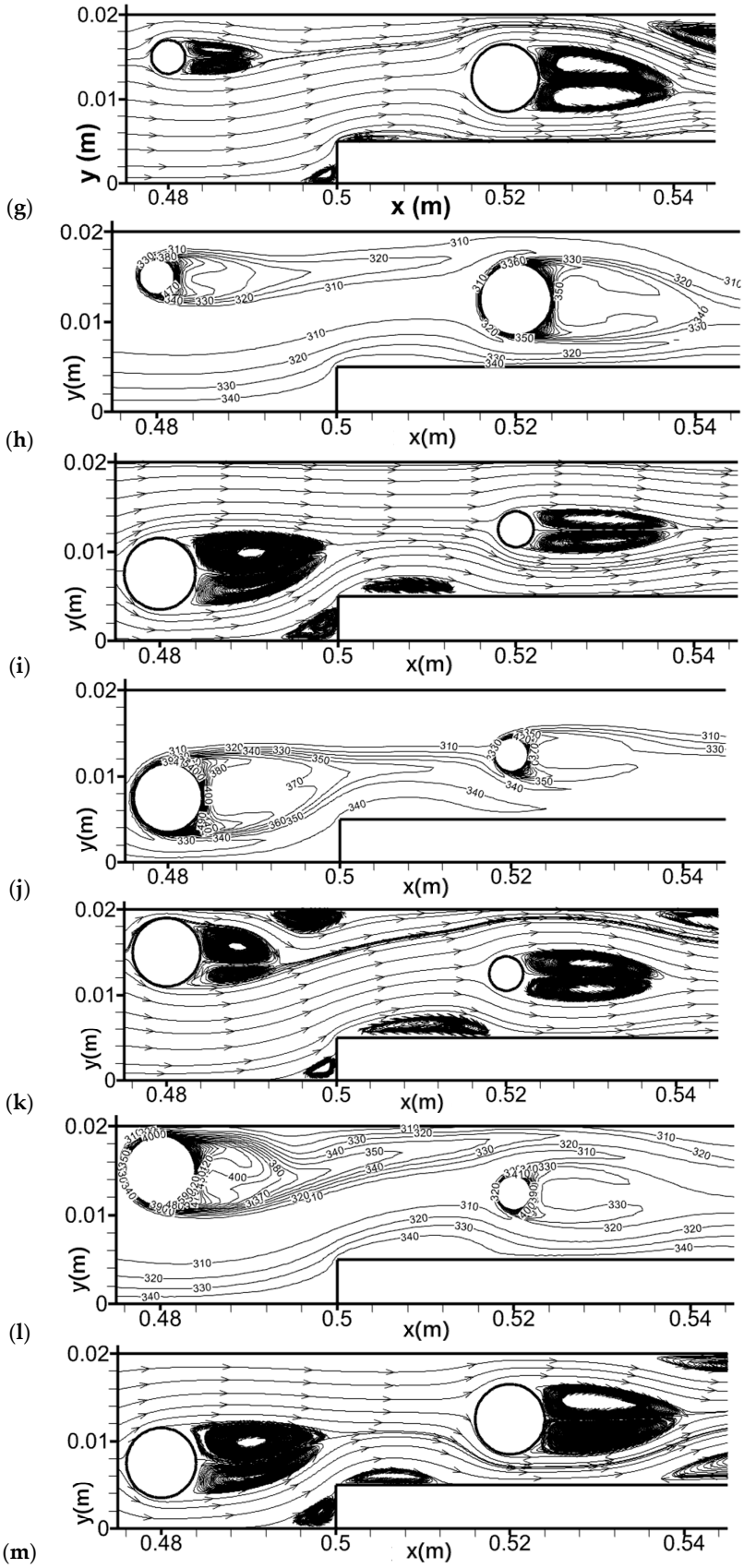


Figure 5. *Cont*.

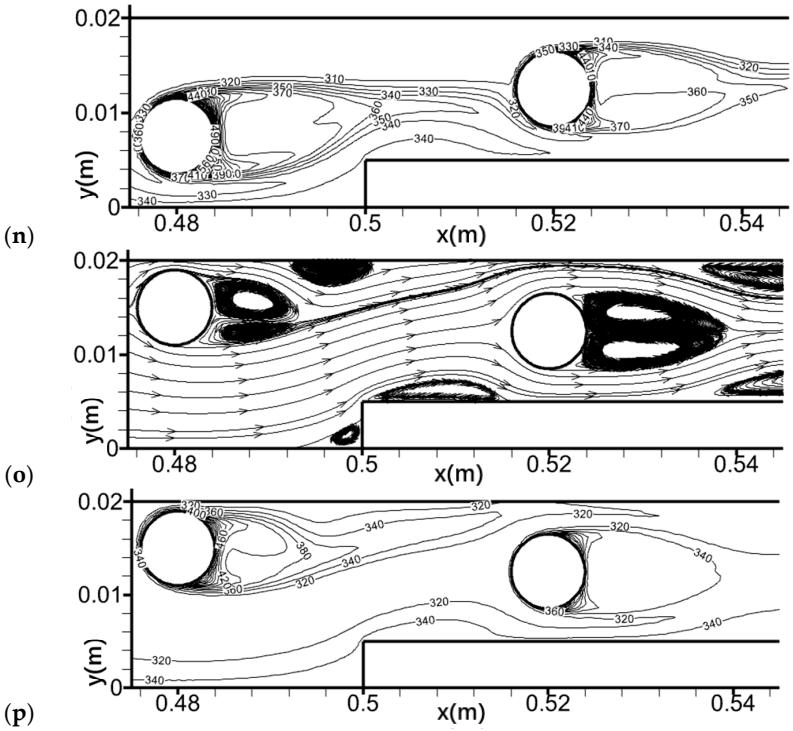


Figure 5. Steam line (which is shown with arrowhead) and isothermal contour for Re = 800. $d_1 = d_2 = 0.2H$, $y_1 = 0.375H$ for (**a**,**b**), and $y_1 = 0.75H$ for (**c**,**d**). Steam line (which is shown with arrowhead) and isothermal contour for $Re = 800$. $d_1 = 0.2$H and $d_2 = 0.4H$ from (**e**–**h**) and from (**i**–**l**), $d_1 = 0.4H$. $Re = 800$. From (**i**–**n**) $d_1 = 0.4H$. $Re = 800$. $y_1 = 0.75H$ from (**o**,**p**) and $d_1 = 0.4H$.

The effect of the vertical position of cylinder c_1 is reported in Figures 7 and 8 for laminar and turbulent flow, respectively. The figure illustrates that when c_1 is at $y_1 = 0.375H$, the wake of c_1 reduces the flow velocity between the step and cylinder c_2. As a result, the heat transfer of the lower half reduces and deviates from the upper half of c_2, which has higher heat transfer due to the higher flow velocity. The heat transfer of the lower half of c_2 gets affected by the heat carried from c_1 when it is at $y_1 = 0.375H$; this phenomenon is the major reason the low Reynolds number has less heat transfer on the lower half of c_2, especially in laminar flow. Meanwhile, in the case of high Re, the deviation in the local Nusselt number of the lower half of c_2 is due to deflected flow from the c_1 because at high turbulent flow, more heat transfer happens at the hot lower wall (at constant temperature) than at the cylindrical obstacle. A turbulent flow velocity profile around c_1 affects the heat transfer of c_2 more than the temperature profile from c_1. That is the reason for the large difference in Figure 8a,b where, as the difference is very low in the case of Figure 7a,b, the diameter of c_1 significantly affects the velocity profile but not the temperature contour. That is why for a larger diameter, there is a high deviation of heat transfer in the lower and upper halves of c_2 when c_1 is at $y_1 = 0.375H$ and turbulent flow. This can even be proven by comparing Figures 9a and 10a.

When $y_1 = 0.75H$, the wake of c_1 is pushed towards the upper half of c_2 due to the deviated flow from the step. As a result, the upper half of c_2 is affected by the heat transfer of c_1, whereas the lower half is majorly affected by the heat transfer from DFFS. In the case of laminar flow, the heat transfer of the upper half and lower half of cylinder c_2 is almost the same when $y_1 = 0.75H$, unlike turbulent flow at $y_1 = 0.375H$. This is because at a low Reynolds number, the temperature profile created by c_1 and the lower wall of DFFS are almost the same near c_2.

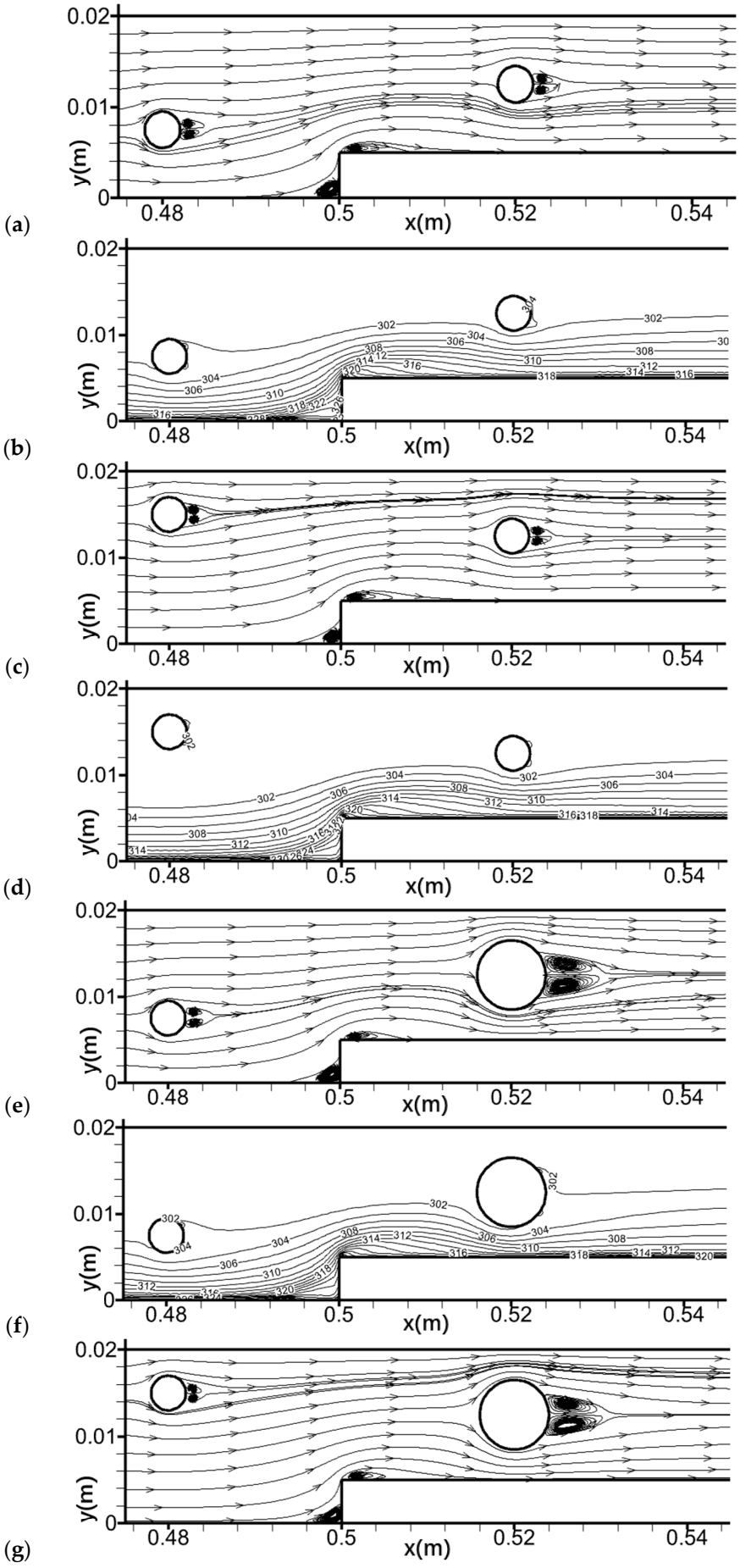


Figure 6. *Cont*.

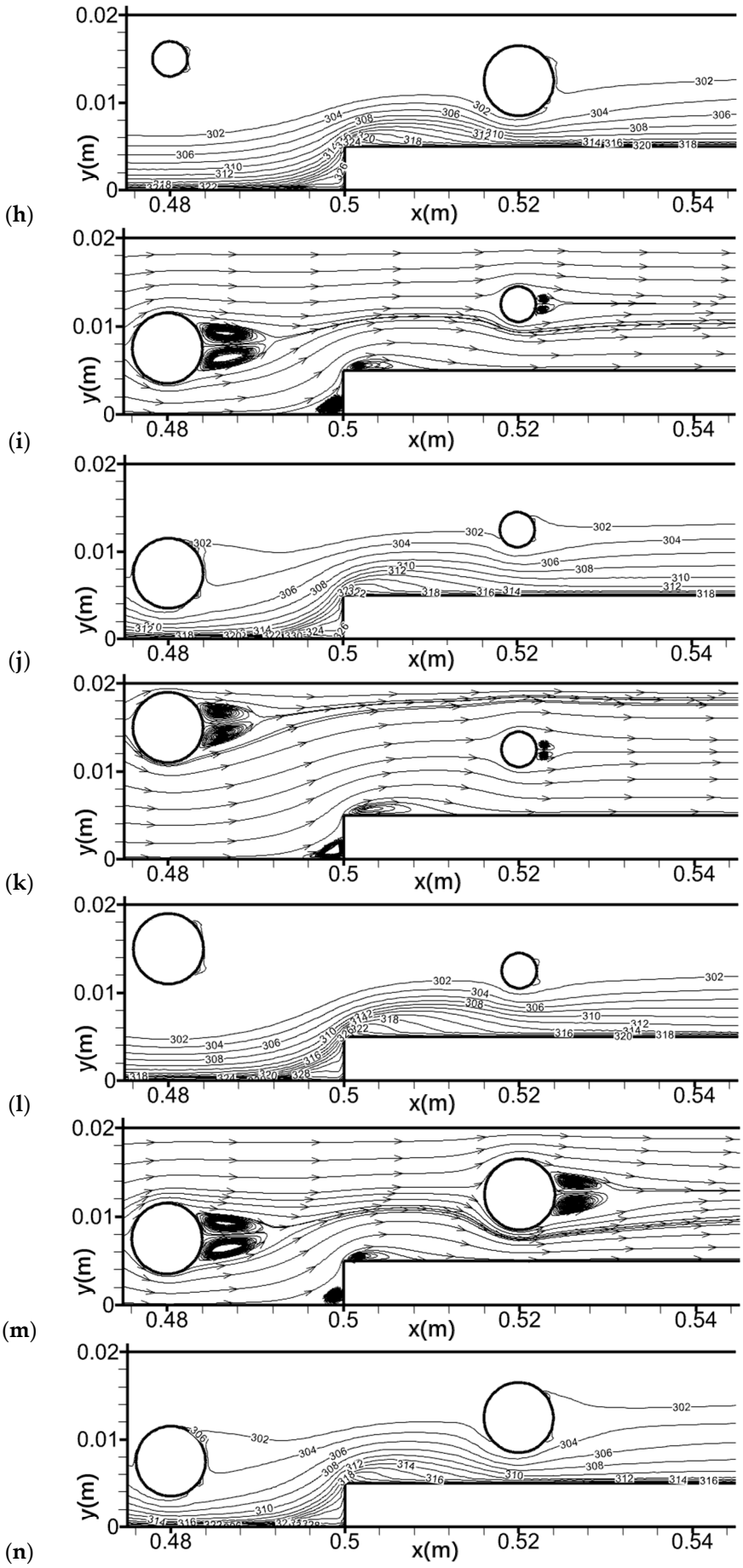


Figure 6. *Cont*.

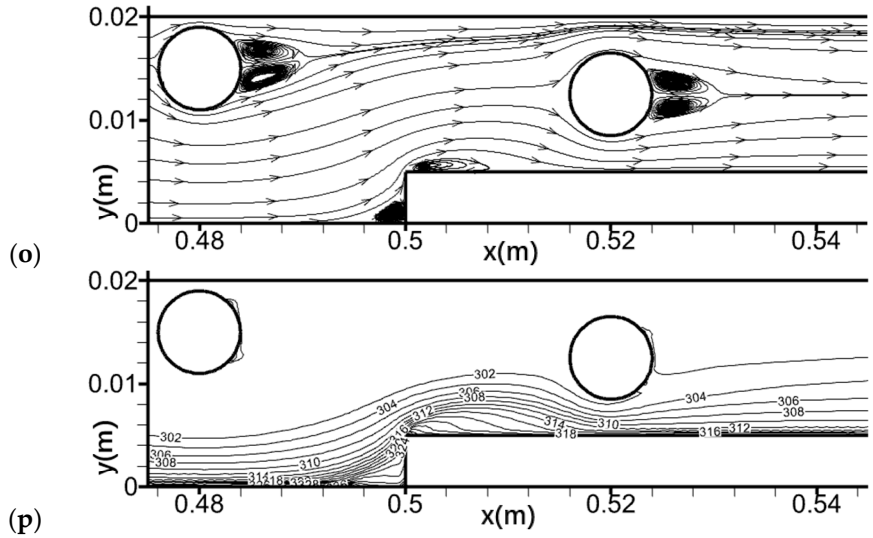


Figure 6. (**a**–**l**) Steam line (which is shown with arrowhead) and isothermal contour for *Re* = 80,000: $d_1 = d_2 = 0.2H$. *Re* = 80,000: From (**m**–**p**) $d_1 = d_2 = 0.4H$.

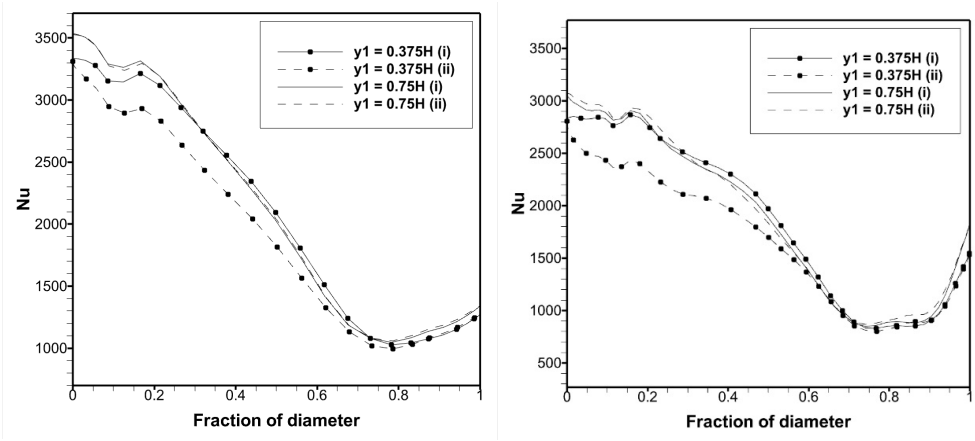


Figure 7. *Re* = 800; (**a**) $d_1 = d_2 = 0.2H$; (**b**) $d_1 = d_2 = 0.4H$.

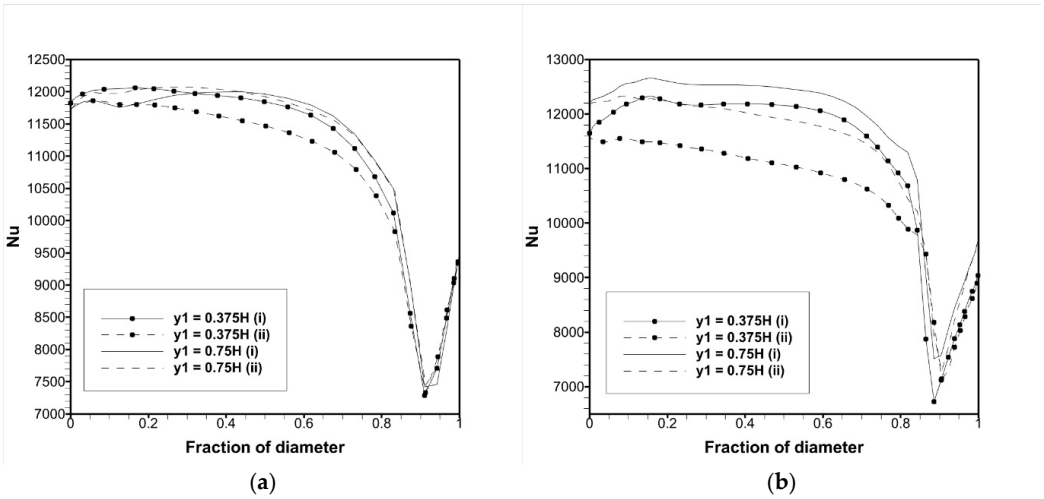


Figure 8. *Re* = 80,000; (**a**) $d_1 = d_2 = 0.2H$; (**b**) $d_1 = d_2 = 0.4H$.

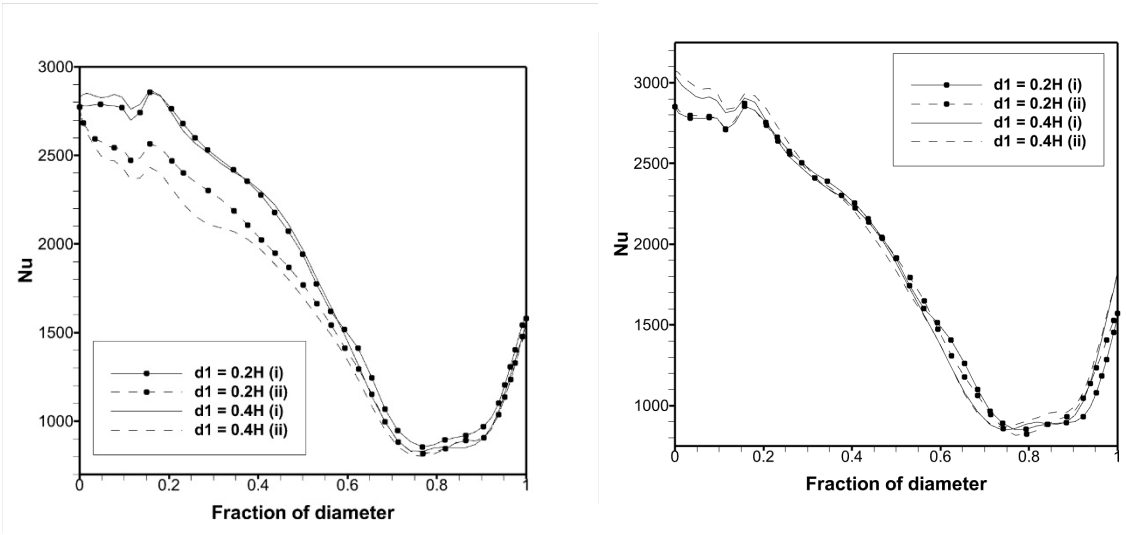


Figure 9. $d_2 = 0.4H$, $Re = 800$, (**a**) $y_1 = 0.375H$; (**b**) $y_1 = 0.75H$.

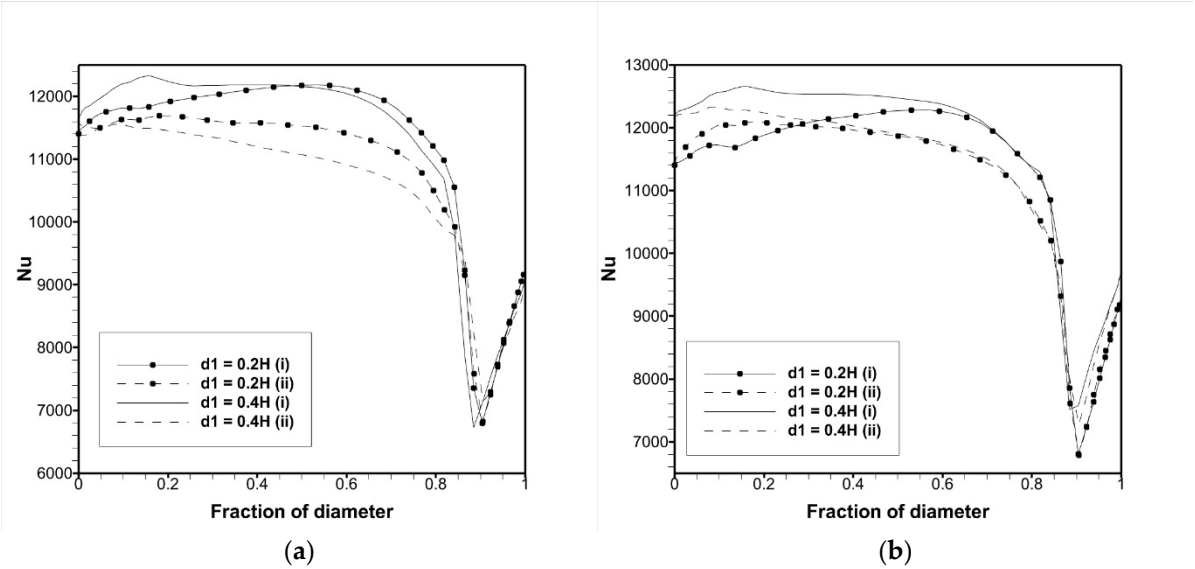


Figure 10. $d_2 = 0.4H$, $Re = 80{,}000$, (**a**) $y_1 = 0.375H$; (**b**) $y_1 = 0.75H$.

It observed that if d_2 is less than the step height, i.e., $d_2 = 0.2H$, the heat transfer at the initial diameter fraction will be based on the vertical position of cylinder c_1, whereas if d_2 is more than the step height, then the heat transfer at the initial diameter fraction will be based on d_1. For $c_2 = 0.4H$, the initial heat transfer is higher for $d_1 = 0.4H$ in all cases, whereas in $d_2 = 0.2H$, the initial heat transfer is higher for $d_1 = 0.4H$ if $y_1 = 0.75H$, and $d_1 = 0.2H$ will have more initial heat transfer when $y_1 = 0.375H$. This is because the flow around c_2 is interrupted by both the step and cylinder c_1 diameter, whereas if d_2 is more than the step height, then the flow will be majorly interrupted by cylinder d_1. When c_1 is at $y_1 = 0.375H$, the wake of c_1, along with recirculation over the first step, creates a high temperature near c_2, which results in lower heat transfer; this is mainly if c_2 is less than the step height. When d_1 increases, the recirculation wake also increases, which decreases the heat transfer initial diameter fraction of cylinder c_2. On the other hand, when c_1 is at $y_1 = 0.75H$, the created wake gets pushed over c_2's upped half by deflected flow from the step. Thus, a larger c_1 will have more heat transfer.

Figures 8, 10 and 11 show that for a high Reynolds number cases and Figures 9 and 12 show low Reynolds number results. The local Nu along the cylinder is shown in Figure 8 for *Re* = 80,000 (Figures 8, 10 and 11). When the diameter of both cylinder is small as 0.2H, the local Nu varies for different step height and wen the diameter is increased significant variations is recorded. This trend is more significant at low Re = 800 (Figures 9 and 10). If c_1 is less than the step height and $y_1 = 0.75H$, then initially, up to some point of diameter fraction, the lower half has higher heat transfer than the upper half of c_2, and along the flow, the heat transfer of the upper half of cylinder c_2 dominates gradually. In this case, the heat transfer of the upper half of cylinder c_2 should be higher than the lower half of c_2 since the temperature profile developed by the bottom wall of DFFS affects the c_2 cylinder's lower half, but because the flow diverted by cylinder c_1 goes close to the upper half of cylinder c_2, the heat transfer of the upper half of c_2 reduces initially and after some distance because as heat transfer over lower half retards, the upper half dominates. In the case of c_1 being larger than the step height, the flow goes away (comparatively) from c_2; thus, heat transfer happens normally.

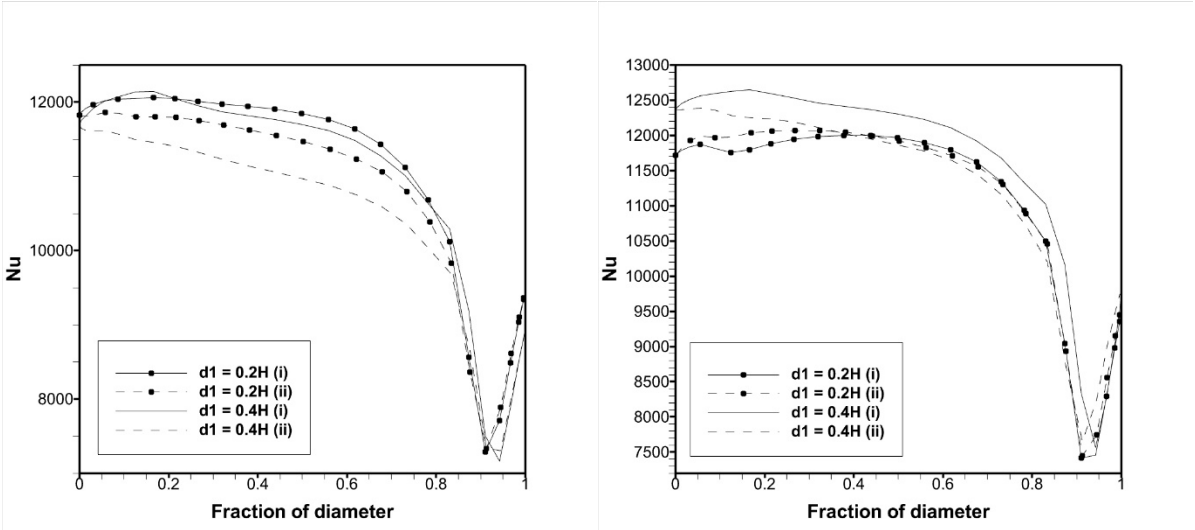


Figure 11. $d_2 = 0.2H$, Re = 80,000, (**a**) $y_1 = 0.375H$; (**b**) $y_1 = 0.75H$.

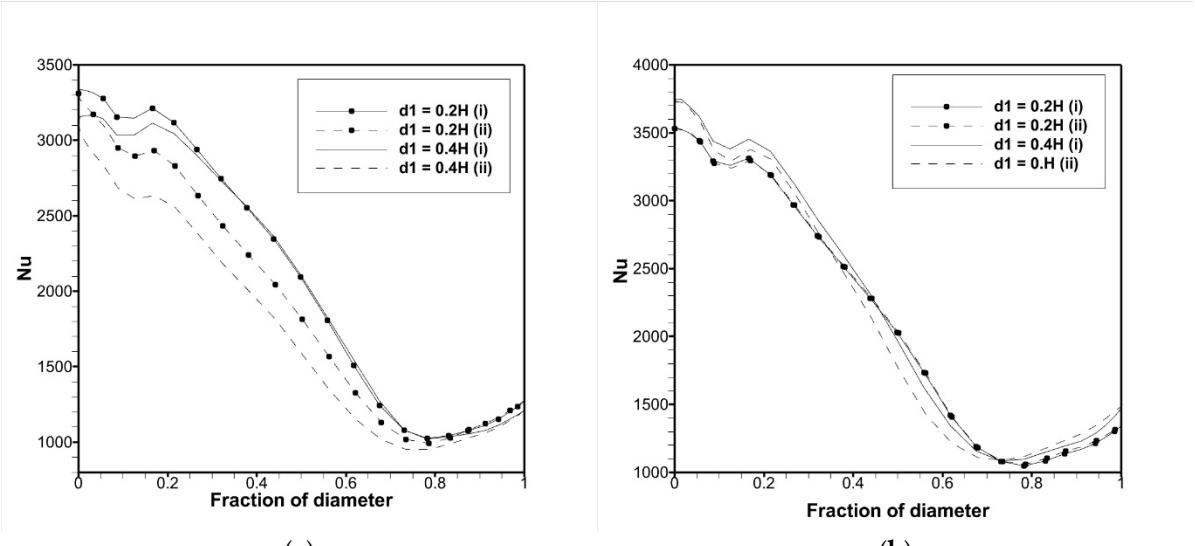


Figure 12. $d_2 = 0.2H$, Re = 800, (**a**) $y_1 = 0.375H$; (**b**) $y_1 = 0.75H$.

Towards the end of the diameter fraction, heat transfer of the lower and upper halves dominate each other. Then, at the very end, the overlap is due to the recirculation created by the wake of the cylinder. The irregular temperature profile near the cylinder toward the end of the diameter fraction creates an asymmetric local heat transfer, which makes the lower and upper halves dominate over each other.

From Tables 4–7 the summary of all the cases reported for average Nusslet number. The average Nusselt number for $d_1 = 0.2H$ size cylinder case is shown in Table 4.

Table 4. Average Nusselt number: Effect of d_1 while $d_2 = 0.2H$ and $y_1 = 0.75H$.

Re	Nu_1 ($d_1 = 0.2H$)	Nu_2 ($d_1 = 0.2H$)	$Nu_1 - Nu_2$
200	1126.201	1107.933	18.267
800	2232.531	2163.047	69.483
20,000	6789.945	6565.587	244.358
80,000	11,264.33	10,927.510	336.822

Table 5. Average Nusselt number: Effect of d_1 while $d_2 = 0.2H$ and $y_1 = 0.375H$.

Re	Nu_1 ($d_1 = 0.2H$)	Nu_2 ($d_1 = 0.2H$)	$Nu_2 - Nu_1$
200	901.589	925.717	24.128
800	1930.573	2010.461	79.887
20,000	6279.666	6407.559	127.893
80,000	10,567.57	10,801.25	233.675

Table 6. Average Nusselt number: Effect of d_2 while $d_1 = 0.2H$ and $y_1 = 0.75H$.

Re	Nu_1 ($d_2 = 0.4H$)	Nu_2 ($d_2 = 0.2H$)	$Nu_2 - Nu_1$
200	941.372	1107.933	166.561
800	1914.063	2163.047	248.983
20,000	6517.293	6565.587	48.294
80,000	10,916.801	10,927.510	10.708

Table 7. Average Nusselt number: Effect of d_2 while $d_1 = 0.2H$ and $y_1 = 0.375H$.

Re	Nu_1 ($d_2 = 0.4H$)	Nu_2 ($d_2 = 0.2H$)	$Nu_2 - Nu_1$
200	866.750	997.007	130.256
800	1861.821	2077.461	215.6396
20,000	6333.601	6359.787	26.185
80,000	10,768.25	10,801.25	33.0005

Its value is increased when Re is increased. But the difference between two cylinder is around 1.5% to 4 % only (Tables 5–7). Also, it is observed that for laminar range such increase is high when compare to turbulent. Average Nusselt number is decreased when position of the cylinder moves from $0.75H$ to $0.375H$.

4. Conclusions

A numerical study was conducted on the double forward-facing step (DFFS) with a cylindrical obstacle and the results were plotted for cylinder c_2, which show the effect of cylinder c_1 on the heat transfer of c_2. The study compared the results of different Reynolds numbers (laminar and turbulent flow), two different cylinder diameters, and two different positions of cylinder d_1. From the investigation, it was observed that a high *Re* leads to fewer recirculation zones than a low Reynolds number; this is the major reason for high *Re* having more heat transfer than low *Re*, as recirculation zones are zones of temperature accumulation which ultimately reduces heat transfer. To have equal heat transfer over the

upper and lower halves of c_2, c_1 should be near the top wall of the DFFS, and flow should be laminar with low *Re*. Toward the rear of c_2, irregular heat transfer occurs due to the wake of c_2, which recirculates. When d_2 is lower than the step height, c_1 being near the top wall will always give more heat transfer of c_2, whereas if d_2 is greater than the step height then a larger diameter d_1 will have a greater heat transfer effect on cylinder c_2.

For the laminar flow of *Re* = 800, a larger difference in heat transfer of the upper and lower halves was observed for $d_1 = 0.4H$ and c_1 near the bottom wall of the DFFS; i.e., at $y_1 = 0.375H$, the differences for $d_2 = 0.2H$ and $0.4H$ are about 6.3% and 5.5% of the total heat transfer of c_2, respectively. It is clear that a larger d_2 has a smaller difference in heat transfer. Meanwhile, in the case of $d_1 = 0.2H$, it is noted that larger d_2 has a larger difference in heat transfer for $y_1 = 0.375H$, which is vice versa of d_1—$0.4H$. For $d_1 = 0.2H$ and $y_1 = 0.375H$, the difference in heat transfer of the lower and upper halves of $d_2 = 0.2H$ is 3.3% of the total heat transfer, whereas for $d_2 = 0.4H$, it is 4.2%. In all the different combinations of d_1 and d_2 for low Reynolds number, it was identified that $y_1 = 0.375H$ has almost 4% higher difference than $y_1 = 0.75H$.

In the turbulent flow of *Re* = 80,000, the difference in heat transfer of the upper half and lower half for all the combinations of d_1, d_2, and y_1 is greatly reduced as wake and recirculation reduces. Still, the trend remains the same in all cases of order of heat transfer. If d_2 is less than the step height, which means $d_2 = 0.2H$, then increasing d_1 causes more difference in the heat transfer than increasing the y_1 value, which is less than 1% for change in y_1 whereas more than 1% for change in d_1, and vice versa is true for d_2 being more than the step height ($d_2 = 0.4H$). Average Nusselt number is higher when the cylinders are positioned at $0.75H$ location in the duct.

Author Contributions: Conceptualization, P.R.K., Y.S., G.V.D.P. and J.T.; data curation, P.R.K., Y.S., D.T., T.S. and J.T.; formal analysis, P.R.K., Y.S., G.V.D.P., D.T., T.S. and J.T.; investigation, P.R.K., Y.S., D.T. and T.S.; methodology, P.R.K., Y.S., G.V.D.P., D.T., T.S. and J.T.; resources, P.R.K., Y.S., G.V.D.P., D.T., T.S. and J.T.; software, P.R.K., Y.S. and G.V.D.P.; supervision, P.R.K. and J.T.; validation, P.R.K., Y.S. and G.V.D.P.; visualization, P.R.K., Y.S., G.V.D.P., D.T., T.S. and J.T.; writing—original draft, P.R.K., Y.S., G.V.D.P. and J.T.; writing—review and editing, P.R.K., Y.S., G.V.D.P., D.T., T.S. and J.T. All authors have read and agreed to the published version of the manuscript.

Funding: This research received no external funding.

Data Availability Statement: The raw data supporting the conclusions of this article will be made available by the authors on request.

Conflicts of Interest: Author G. V. Durga Prasad was employed by the Newnestech GmbH. The remaining authors declare that the research was conducted in the absence of any commercial or financial relationships that could be constructed as a potential conflict of interest.

References

1. Togun, H.; Ahmadi, G.; Abdulrazzq, T.; Shkarah, A.J.; Kazi, S.N.; Badarudin, A.; Safaei, M.R. Thermal performance of nanofluid in ducts with double forward-facing steps. *J. Taiwan Inst. Chem. Eng.* **2015**, *47*, 28–42. [CrossRef]
2. Kherbeet, A.S.; Mohammed, H.A.; Munisamy, K.M.; Saidur, R.; Salman, B.H.; Mahbubul, I.M. Experimental and numerical study of nanofluid flow and heat transfer over microscale forward-facing step. *Int. Commun. Heat Mass Transf.* **2014**, *57*, 319–329. [CrossRef]
3. Albdoor, A.K.O.; Kamel, M.S.; Farhood, A.K. Characteristics of Heat Transfer and Fluid Flow over a Double Forward Facing Step. Available online: https://www.academia.edu/34008762/Characteristics_of_Heat_Transfer_and_Fluid_Flow_over_a_Double_Forward_Facing_Step (accessed on 1 January 2025).
4. Yılmaz, I.; Öztop, H.F. Turbulence forced convection heat transfer over double forward facing step flow. *Int. Commun. Heat Mass Transf.* **2006**, *33*, 508–517. [CrossRef]
5. Oztop, H.F.; Mushatet, K.S.; Yılmaz, İ. Analysis of turbulent flow and heat transfer over a double forward facing step with obstacles. *Int. Commun. Heat Mass Transf.* **2012**, *39*, 1395–1403. [CrossRef]

6. Janani, M.; Prakash, D.; Harini, E.; Harish, T. Enhancement of heat transfer over Double forward facing step with square obstacle through Taguchi's Optimization techniques. *Int. J. Eng.* **2017**, *30*, 1253–1259.
7. Barman, A.; Dash, S.K. Effect of obstacle positions for turbulent forced convection heat transfer and fluid flow over a double forward facing step. *Int. J. Therm. Sci.* **2018**, *134*, 116–128. [CrossRef]
8. Togun, H.; Shkarah, A.J.; Kazi, S.N.; Badarudin, A. CFD Simulation of Heat Transfer and Turbulent Fluid Flow over a Double Forward-Facing Step. *Math. Probl. Eng.* **2013**, *2013*, 895374. [CrossRef]
9. Sture, H.; Gyr, A.; Kinzelbach, W. Laminar separation on a forward facing step. *Eur. J. Mech. B/Fluids* **1999**, *18*, 675–692.
10. Werner, H.; Wengle, H. Large eddy simulation of turbulent flow over a square rib in a channel. In *Advances in Turbulence*, 2nd ed.; Fernholz, H.H., Fiedler, H.E., Eds.; Springer: Berlin/Heidelberg, Germany, 1989; pp. 418–423.
11. Freitas, C.J.; Street, R.L. Non-linear transient phenomena in a complex recirculation flow: A numerical investigation. *Int. J. Numer. Methods Fluids* **1988**, *8*, 769–802.
12. Dimaczek, G.; Kessler, R.; Martinuzzi, R.; Tropea, C. The flow over two-dimensional surface mounted obstacles at high Reynolds numbers. In *7th Symposium on Turbulent Shear Flows*; Stanford University: Stanford, CA, USA, 1989; pp. 10.1.1–10.1.6.
13. Mohammeda, H.A.; Al-aswadi, A.A.; Shuaib, N.H.; Saidur, R. Convective heat transfer and fluid flow study over a step using nanofluids: A review. *Renew. Sustain. Energy Rev.* **2011**, *15*, 2921–2939.
14. Abu-Mulaweh, H.I. A review of research on laminar mixed convection flow over backward- and forward-facing step. *Int. J. Therm. Sci.* **2003**, *42*, 897–909. [CrossRef]
15. Rao, A.N.; Zhang, J.; Minelli, G.; Basara, B.; Karajnovic, S. Qualitative assessment if the bi-stable states in the wake of a finite width double forward facing step. *J. Wind. Eng. Ind. Aerodyn.* **2019**, *186*, 241–249. [CrossRef]
16. McQeen, T.; Burton, D.; Sheridan, J.; Thompson, M.C. The double backward facing step: Effect of forcing on interacting separated flow regions. *J. Fluid Mech.* **2022**, *946*, A9. [CrossRef]
17. Chauhan, M.K.; Dutta, S.; Gandhi, B.K. Wake flow modification behind a square cylinder using control rods. *J. Wind Eng. Ind. Aerodyn.* **2019**, *184*, 342–361. [CrossRef]
18. Abbasi, W.S.; Ismail, S.; Nadeem, S.; Rahman, H.; Majeed, A.H.; Khan, I.; Mohamed, A. Passive control of wake flow behind a square cylinder using a flat plate. *Front. Phys.* **2023**, *11*, 1132926. [CrossRef]
19. Wang, Z.; Zu, S.; Yang, M. Numerical simulation on forced convection over a circular cylinder confined in a sudden expansion channel. *Int. Commun. Heat Mass Transf.* **2018**, *91*, 48–56. [CrossRef]
20. Xie, W.A.; Xi, G.N. Geometry effect on flow fluctuation and heat transfer in unsteady forced convection over backward and forward facing step. *Energy* **2017**, *132*, 49–56. [CrossRef]
21. Lekkala, M.R.; Latheef, M.; Jung, J.H.; Coraddu, A.; Zhu, H.; Srinil, N.; Lee, B.-H.; Kim, D.K. Recent advances in understanding the flow over bluff bodies with different geometries at moderate Reynolds numbers. *Ocean Eng.* **2022**, *261*, 111611. [CrossRef]
22. Narayanan, B.A.; Lakshmanan, G.; Mohammad, A.; Kishore, V.R. Laminar Flow over a Square Cylinder Undergoing Combined Rotational and Transverse Oscillations. *J. Appl. Fluid Mech.* **2021**, *14*, 259–273. [CrossRef]
23. Zhang, L. Numerical Simulation of Flows past a Circular and a Square Cylinder at High Reynolds Number, and a Curved Plate in Transitional Flow. Master's Thesis, McKelvey School of Engineering, St. Louis, MO, USA, 2017.
24. Bot, P.; Rabaud, M.; Thomas, G.; Lombardi, A.; Lebert, C. Sharp Transition in the Lift Force of a Fluid Flowing Past Nonsymmetrical Obstacles: Evidence for a Lift Crisis in the Drag Crisis Regime. *Phys. Rev. Lett.* **2016**, *117*, 234501. [CrossRef]
25. Xu, Z.; Wu, S.; Wu, X.; Xue, W.; Wang, F.; Gao, A.; Zhang, W. Analysis of Flow Characteristics around a Square Cylinder with Boundary Constraint. *Water* **2023**, *15*, 1507. [CrossRef]
26. Rastan, M.R.; Sohankar, A.; Doolan, C.; Moreau, D.; Shirani, E.; Alam, M.M. Controlled flow over a finite square cylinder using suction and blowing. *Int. J. Mech. Sci.* **2019**, *156*, 410–434. [CrossRef]
27. Launder, B.E.; Spalding, D.B. The Numerical Computation of Turbulent Flows. In *Numerical Prediction of Flow, Heat Transfer, Turbulence and Combustion*; Elsevier: Amsterdam, The Netherlands, 1983; pp. 96–116. [CrossRef]

Disclaimer/Publisher's Note: The statements, opinions and data contained in all publications are solely those of the individual author(s) and contributor(s) and not of MDPI and/or the editor(s). MDPI and/or the editor(s) disclaim responsibility for any injury to people or property resulting from any ideas, methods, instructions or products referred to in the content.